European Journal of Medicinal Chemistry 282 (2025) 117107

Contents lists available at ScienceDirect

European Journal of Medicinal Chemistry

journal homepage: www.elsevier.com/locate/ejmech

Research paper

Design and functional studies of xylene-based cyclic mimetics of SOCS1 protein

Alessia Cugudda [a,1], Sara La Manna [a,1], Marilisa Leone [b], Marian Vincenzi [b], Daniela Marasco [a,b,*]

[a] Department of Pharmacy - University of Naples Federico II, 80131, Naples, Italy
[b] Institute of Biostructures and Bioimaging - CNR, 80131, Naples, Italy

ARTICLE INFO

Keywords:
Mimetic peptides
Cytokine signaling
JAK-STAT
SOCS1
Cyclic peptides

ABSTRACT

Peptidomimetics of Suppressors of cytokine signaling 1 (SOCS1) protein demonstrated valid therapeutic potentials as anti-inflammatory agents. Indeed, SOCS1 has a small kinase inhibitory region (KIR) primarily involved in the inhibition of the JAnus Kinase/Signal Transducer and Activator of Transcription (JAK/STAT) pathway Herein, on the basis of previous investigations on a potent mimetic of KIR-SOCS1, named PS5, we designed and evaluated the SAR (Structure Activity Relationship) features of two xylene-based macrocycles analogues of PS5. These novel compounds bear thiol-xylene linkages with mono- and bi-cyclic scaffolds: they were *in vitro* functionally investigated toward JAK2 catalytic domain, as ligands with microscale thermophoresis (MST) and as inhibitors through LC-MS analyses. To evaluate structural properties Circular Dichroism (CD) and Nuclear Magnetic Resonance (NMR) spectroscopies were employed along with serum stability assays. Results indicated that a monocycle scaffold is well-tolerated by PS5 sequence enhancing the affinity toward the kinase with a K_D in the low micromolar range and providing consistent inhibitory effects of the catalytic activity, which were evaluated for the first time in the case of SOCS1 mimetics. Conformationally, the presence of xylene scaffold affects the flexibility of the compounds and their stabilities to proteases degradation. This study contributes to the understanding of the factors necessary for accurately mimicking the inhibitory mechanism of SOCS1 protein towards JAK2 and to the translation of proteomimetics into drugs.

1. Introduction

Suppressor Of Cytokine Signaling (SOCS) 1 protein is a critical negative regulator of cytokine signaling and required to protect against an excessive inflammatory response [1]. Among SOCS family members, SOCS1 exhibits the broadest spectrum of cytokines regulation [2]: its expression is induced by many cytokines, through a classical negative feedback loop mechanism [3]. Genetic deletion of SOCS1 results in uncontrolled cytokine signaling and neonatal mortality [4], with inflammatory immune infiltrates in multiple organs [4]. SOCS1 exerts a primary role in immune homeostasis in humans and its haploinsufficiency causes a dominantly inherited predisposition to early onset autoimmune diseases related to cytokine hypersensitivity of immune cells [5]. This effect is associated with a series of *in vitro* and *in vivo* immune abnormalities consistent with lymphocyte hyperactivity. SOCS1 deficiency increases the expression of Nuclear factor erythroid 2-related factor 2 (NRF2) which is a tumor suppressor in normal cells but becomes an oncoprotein in liver cancer cells and confers resistance to oxidative stress. Hence, controlling the oxidative stress response, is an important tumor suppression mechanism of SOCS1 [6]. Investigations into the tumor suppressive mechanisms of SOCS1 expression highlighted that this protein regulates antitumor immune responses also in a cell-extrinsic manner via direct and indirect mechanisms [7].

SOCS1 over-expression and structural studies indicate that the kinase inhibitory region (KIR) and Src homology 2 (SH2) domain are important for the interaction and inhibition of JAK 1, 2 and TYK2 tyrosine kinases, which are associated with cytokine receptor initiator of the downstream signaling JAK/STAT (Janus kinase (JAK)-signal transducer and activator of transcription (STAT)) [8]. Recently, *in vivo*, the effects of independent mutations of key conserved residues in KIR and SH2 domains, were investigated confirming previous *in vitro* studies: Phe^{58} within KIR and the phosphotyrosine binding capacity of the SH2 domain are essential for the endogenous SOCS1 functions [9]. Phe^{58} occupies a hydrophobic pocket at the interface of the SH2(SOCS1)/JH1(JAK1) and

* Corresponding author. Department of Pharmacy - University of Naples Federico II, 80131, Naples, Italy.
E-mail address: daniela.marasco@unina.it (D. Marasco).
[1] co-first authors.

https://doi.org/10.1016/j.ejmech.2024.117107
Received 25 May 2024; Received in revised form 19 November 2024; Accepted 23 November 2024
Available online 25 November 2024

its mutation suppresses the ability of SOCS1 to inhibit JAK2 [10] while mutation within the phosphotyrosine binding pocket of SH2 domain specifically disrupts SOCS1 interaction with phosphorylated JAK1 (pJAK1). The X-ray structure of JAK1/SOCS1 complex, captured KIR in a "blocked form" where it protrudes toward the substrate-binding site without involving the pTyr binding pocket on the SH2 domain [10]. Hence the confirmation of a critical and non-redundant role of the KIR and SH2 domains in endogenous SOCS1 functions [11]. Indeed, the ability of KIR to bind JAK is independent from the interaction SH2 domain/pTyr and fully consistent with the employment of KIR-mimetics as inhibitors of JAK activity [12]: these compounds demonstrated therapeutic effects in autoimmune and infectious disease models [13]. The immune responses contribute to autoimmunity/inflammation and cancer progression; in particular, a SOCS1-KIR mimetic was recently shown to reduce the pro-inflammatory phenotype in macrophages [14]. Following different medicinal chemistry approaches, in the past we identified a lead peptidomimetic, named PS5 (Fig. 1A and Table S1) [15–17], bearing several substitutions with respect to the wild-type sequence: His^{54}/Cys(Acm), Phe^{55}/Arg and Arg^{56}/Gln. PS5 demonstrated more potent inhibition of JAK/STAT with respect to KIR peptide in cellular and *in vivo* environments [18–22].

The observed preorganization of KIR as pseudosubstrate of JAK1 in the crystal structure [10], suggested the design of cyclic analogues for the presence of several amino acid side chains facing towards the center of the folded protein making them suitable for cyclization. Hence, several analogues of PS5 were designed and analyzed [22–25] and one of them, named *ic*PS5(Nal1) (*ic*: internal cycle), has a lactam bridge between side chains of Asp (naturally occurring at position 52) and Lys (in replacement of Ser^{60}) residues, along with the replacement of Phe^{58} with the non-natural L-1-naphthylalanine [Nal(1')] (Fig. 1B and Table S1). *ic*PS5(Nal1) demonstrated to be a potent binder of JAK2 with the longest lasting biological effects in cells, where it reduced STAT1 migration and NADPH oxidases genes and increased *Sod1* and *Cat* antioxidant genes [26].

With the aim of exploring novel chemical diversity, here we present novel PS5 analogues exhibiting the exchange of the polar amide cyclization strategy with hydrophobic aromatic linkers through mono- and bi-cyclization, following the routes of Chemical Linkage of Peptides onto Scaffolds (CLIPS) strategy [27]. Cyclic compounds (Fig. 1C and D and Table S1) were obtained by combining solid phase peptide synthesis (SPPS) and in solution thiol-linkages. They were characterized in their ability to bind and inhibit JAK2 through MicroScale Thermophoresis (MST) and LC-MS assays, and to resist to proteases degradation in serum stability experiments. Circular Dichroism (CD), and Nuclear Magnetic Resonance (NMR) studies provided conformational insights in their structures. JAK2 was chosen as representative of JAK family to evaluate the efficacy of the peptidomimetics of SOCS1 to recognize it, since the high homology of sequences among the catalytic domains of JAK proteins [28].

2. Results and discussion

2.1. Design of thio-PS5(Nal1) analogues

Previous studies led to the development of a cyclic decapeptidomimetic of KIR of SOCS1, *ic*PS5(Nal1), bearing a lactam bridge between the side chains of the Glu^1 and Lys^9 (linear PS5 numeration) and un-natural building blocks, Cys(Acm) at position 3, and Nal1 in position 7 [26] (Fig. 1B and Table S1), whose SAR features were recently investigated [29]. Although lactam cyclization significantly increased the K_D values with respect to linear counterparts, the amide is positioned above a hydrophobic patch, hence the idea to insert a xylene scaffold linked to the peptide chain by using the same residue positions but through a cysteine alkylation [30]. To this purpose, Glu^1 and Lys^9 were replaced with cysteine and benzylic di- and tri-bromides were cross-linked on the unprotected linear peptides [31]. Indeed, the mono- and bi-cyclization were carried out through the reaction of linear reduced peptide with α-α′-dibromo-m-xylene and 1,3,5-tribromomethylbenzene to obtain thio-monocycle (Fig. 1C) and thio-bicycle PS5(Nal1) (Fig. 1D and Table S1), respectively. The correct linkages were assessed through LC-MS and NMR experiments (see below).

2.2. Affinity toward JAK2 of thio-cyclic PS5(Nal1)

Thio-cyclic analogues of PS5(Nal1) were employed as ligands in MST experiments, to evaluate their ability to recognize JAK2 catalytic domain [32]. In general, JAK proteins share a high degree of sequence homology, particularly in their catalytic domains [28]. MST technique was reported to evaluate the affinity of two JAK2 inhibitors—ruxolitinib and fedratinib. These inhibitors, both FDA-approved for the treatment of adults with intermediate-2 or high-risk primary or secondary myelofibrosis (MF), exhibited KDs of 8.3 μM and 0.8 μM, respectively [33].

Both thio-compounds bound to JAK2, providing dose-response curves of MST signals, reported in Fig. 2A and B, but with different K_D values.

The fitting of experimental data for thio-monocycle PS5(Nal1) allowed an estimation of K_D in the low micromolar range (~7 μM) (Fig. 2A) which resulted 5-fold lower than *ic*PS5(Nal1) (K_D ~36 μM) [26], conversely, the thio-bicycle PS5(Nal1) exhibited a 4-fold higher value (~130 μM) without reaching a complete saturation (Fig. 2B). Clearly, the introduction of a bicyclic scaffold, decreased the ability to recognize JAK2, likely for a partial masking of hot spots of interactions.

To corroborate the employment of MST technique to investigate the ability of our SOCS1 mimetics to act as binders of JAK2 we performed an MST assay using curcumin, a well-known natural JAK2 inhibitor. The results, shown in Fig. S1, provided a K_D value of approximately 90 μM, which is reasonably consistent with the reported IC_{50} value of 15 μM [34].

2.3. Inhibition of JAK2 kinase activity

Both thio-cycles PS5(Nal1) were also investigated in their ability to inhibit *in vitro* the phosphorylation activity of JAK2 toward a known substrate, namely Srctide [35], through LC-MS experiments (Fig. S2 F-G). This is the first time, to the best of our knowledge, that relative IC_{50} values for inhibition of kinase activity of JAK2 by KIR-SOCS1 mimetics are reported. The decrease of the area of the peak of phosphorylated (p-) Srctide, at increasing amounts of thio-cycles as inhibitors (equivalents 0–2, 0–8 for mono-e bi-cycles, respectively), was evaluated, and LC-MS profiles of thio-monocycle PS5(Nal1) are reported in Fig. S2A–E. The variations of the area percentages of p-substrate as function of log (inhibitor) are reported in Fig. 3.

For thio-monocycle PS5(Nal1) the relative half-maximal inhibitory concentration (IC_{50}) was estimated in the low micromolar range, 2.2 ± 0.3 μM, which is quite close to K_D obtained through MST. For the thio-bicycle PS5(Nal1), the relative IC_{50} was (1.0 ± 0.5) $\bullet 10^2$ μM (Fig. 3B), which indicated the lower ability of this compound to act as inhibitor with respect to the monocycle analogue, confirming lower affinity assessed in MST studies. Both relative IC_{50} profiles show steep Hill slopes which may indicate a cooperative mechanism that cannot be excluded.

2.4. Conformational studies by CD and NMR spectroscopy of thio-cyclic PS5(Nal1) analogues

To evaluate the conformational properties of thio-analogues, CD studies were carried out [36] and spectra are reported in Fig. 4.

Thio-analogues of PS5(Nal1) exhibited quite different CD profiles: the bicyclic compound presents the minimum at wavelength lower than 200 nm and a band centered at 230 nm (Fig. 4B): the latter is a peculiar feature of other cyclic PS5 analogues and indicates an aromatic contribution to the structure, enhanced by the naphthyl group, of Nal1, that is absent in the spectrum of its linear counterpart [22,26]. Conversely,

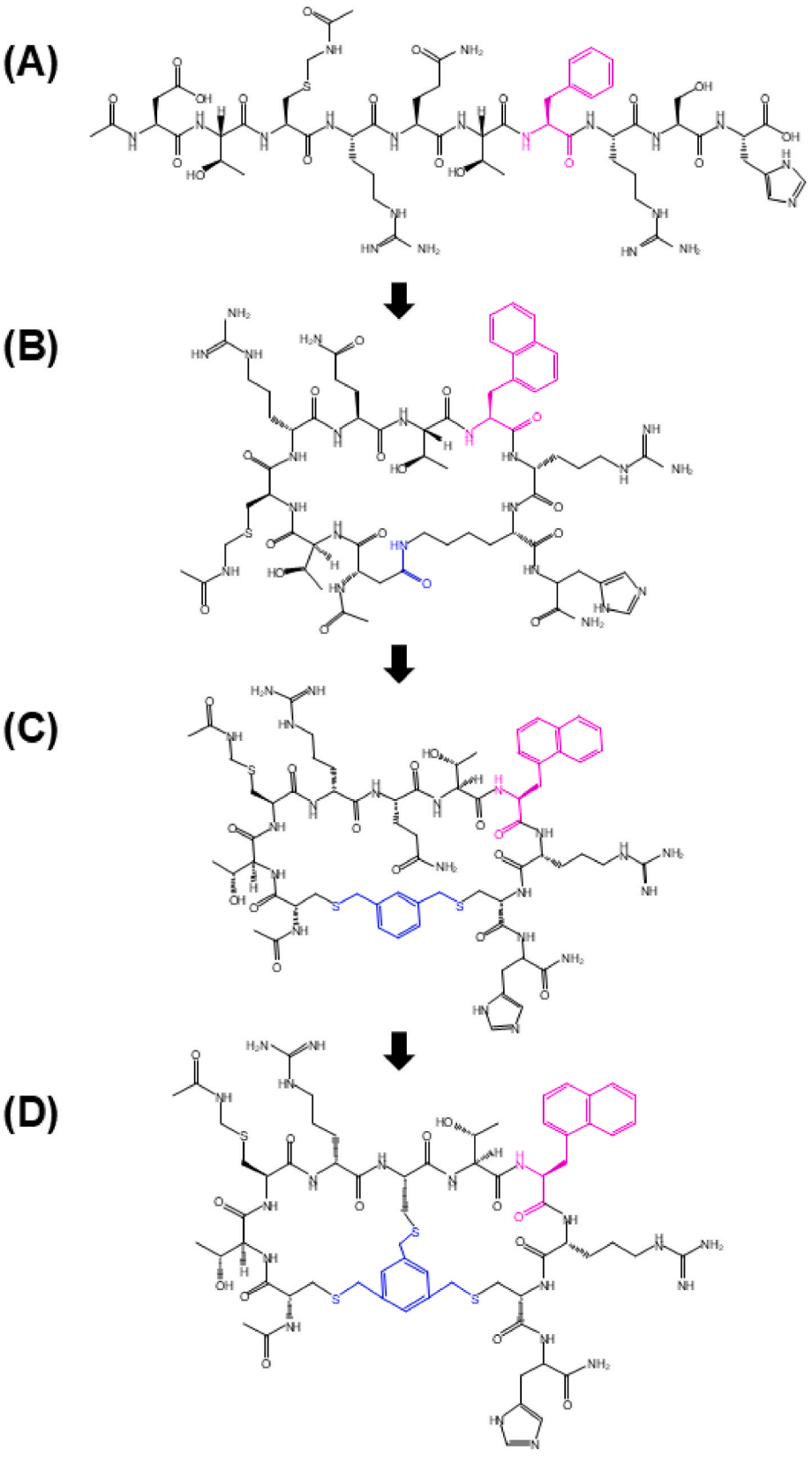

Fig. 1. Design of PS5(Nal1) analogues. Structures of (A) PS5, (B) *ic*PS5(Nal1), (C) thio-monocycle PS5(Nal1) and (D) thio-bicycle PS5(Nal1). The substitution Phe[58]/Nal1 is reported in magenta, lactam and xylene linkages in blue.

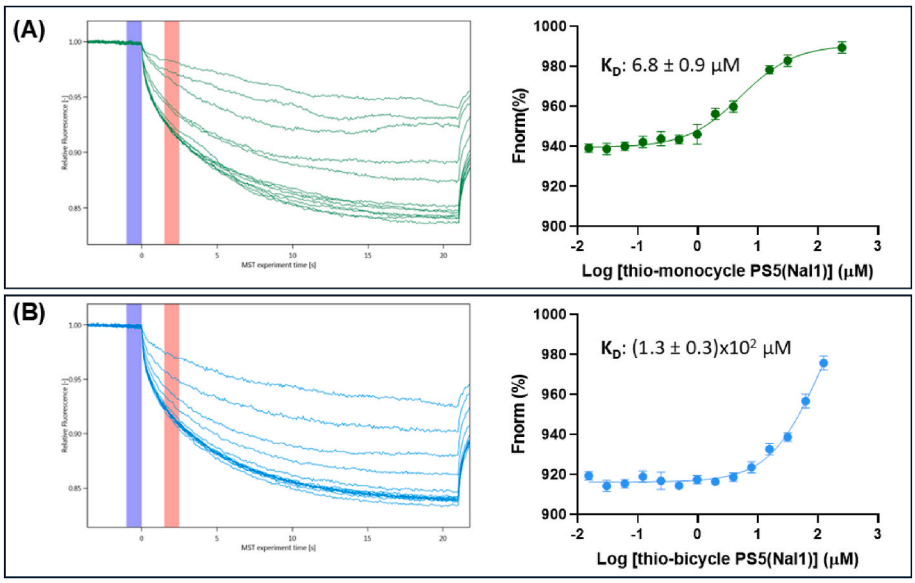

Fig. 2. MST binding assays. (left) thermophoretic traces of MST for the binding to JAK2 (right) binding isotherms for MST signals versus ligand concentrations of (A) thio-monocycle PS5(Nal1) and (B) thio-bicycle PS5(Nal1). The data are the average of two experiments.

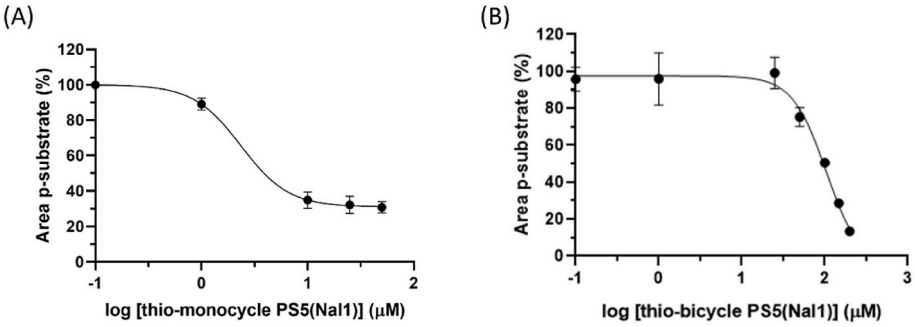

Fig. 3. Area percentages of p-Srctide values at different concentrations of (A) thio-monocycle PS5(Nal1) (B) thio-bicycle PS5(Nal1), function log(inhibitor) vs response - - Variable slope (four parameters). Data are the average of two distinct experiments. Mean ± SD. 100 % was assumed the area of p-Srctide in the absence of the inhibitor.

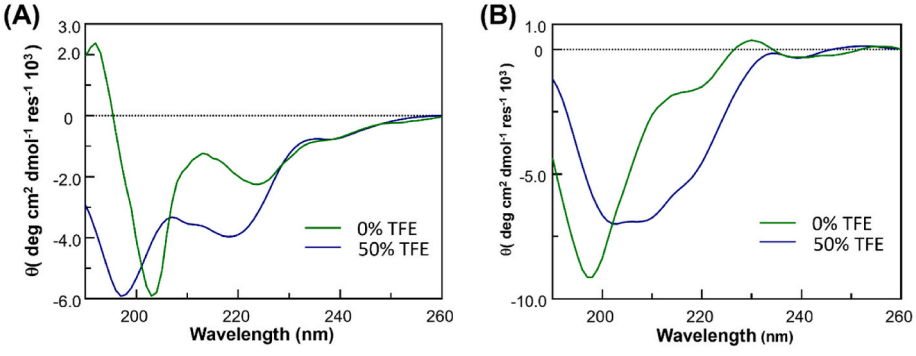

Fig. 4. Overlay of CD spectra of (A) thio-monocycle PS5(Nal1); (B) thio-bicycle PS5(Nal1) compounds.

thio-monocycle PS5(Nal1) does not present the aromatic band rather two minima, at ~224–203 nm and a maximum at 190 nm, with a $\theta_{224/203nm}$ distinctly smaller than unity (0.38) (Fig. 4A). The addition of TFE (2,2,2-trifluoroethanol) (50 % (v/v)) determines variations in the CD spectrum without bringing an increase in the content of canonical secondary structures with respect to the thio-monocycle PS5(Nal1). Indeed, the shift of the above-mentioned minima towards lower wavelengths, ~218 and ~197 nm, respectively, with an $\theta_{218/197nm}$ of 0.67 (Fig. 4A), suggests the absence of helical content in the structure, as confirmed by the deconvolution of the CD spectra (Table S2). Conversely, in the case of thio-bicycle PS5(Nal1), the presence of TFE causes the disappearance of the aromatic band and the emergence of a broad band centered at 210 nm, indicating a significant β-content in the structure.

Thio-monocycle PS5(Nal1) was further characterized by 1D [^{1}H] and 2D [^{1}H, ^{1}H] NMR spectroscopy in aqueous buffer and in the presence of

TFE (Figs. S3 and S4). From the comparison of 1D [^{1}H] spectra (Fig. S3A), TFE co-solvent was unable to improve spectral dispersion and increase the content of ordered secondary structures, in line with CD data. In the H_N/aromatic protons correlation region of 2D spectra, only a reduced set of cross-peaks was observed (Fig. S3B and C) indicating the solvent exposure of amide H_N protons. The lack of a significant number of NOE or ROE contacts and of relevant correlations in the TOCSY spectra (Fig. S3B and C), hampered unambiguous resonance assignments (Table S3) even if, in the presence of TFE, the correlations between cysteines and aromatic protons were evident and confirmed the correct cyclic arrangement (Figs. S3C and S4).

2.5. Serum stability of thio-cyclic analogues

Serum stability assays were carried out to evaluate the proteolytic stability of thio-cyclic analogues of *ic* PS5(Nal1). In Fig. 5, the degradation profiles of the novel compounds are reported, in comparison with *ic*PS5(Nal1). Both thio-analogues appeared more prone to degradation over time with respect to *ic*PS5(Nal1) even if, after 30 h, both compounds are still present with a percentage of 25 %.

3. Discussion

In general, JAK inhibitors may have therapeutic benefits in dampening vascular inflammation and allogeneic leukocyte activation [37] and even if, actually, several small JAK inhibitors are clinically employed, they can display low selectivity [8]. Herein we followed a different approach by designing mimetics of SOCS1: some of them, recently, demonstrated protective roles against pathological glomerular changes in mesangial proliferative glomerulonephritis (MsPGN), by reducing macrophage infiltration and inhibiting macrophage polarization to the M1 phenotype [38]. This defensive function was also assessed in the inhibition of the inflammatory signatures associated with TLR7/IFNγ stimulation and IFNγ-induced endothelial cell (EC): antigen-presenting capacity was prolonged after cytokine withdrawal.

In the context of KIR-SOCS1 analogues, in this study, we employed a CLIPS-based medicinal chemistry approach to investigate the potential of cyclic PS5(Nal1) analogues containing a xylene scaffold with di- and ter-thio-links to the peptide. This led to the discovery of monocycle and bicycle PS5(Nal1) analogues (Fig. 1). These two novel compounds were then subjected to structural and functional characterization, and their ability to inhibit JAK2 kinase was quantified in terms of relative IC_{50}. For these analogues, the type of cyclic arrangement has a significant impact on the capacity to recognize the JAK2 protein. Indeed, MST assays demonstrated that the bicyclic scaffold reduces this ability by approximately 20-fold, likely due to the masking or losing of crucial hot spots for the interaction. Conversely, the monocyclic derivative demonstrated enhanced affinity towards JAK2 with respect to *ic*PS5 (Nal1) in the low micromolar range and exhibited a relative IC_{50} value in the same range, indicating the specificity of the mechanism of action (MOA). The presence of an unnatural xylene scaffold on a short and not pre-organised peptide backbone strengthened the lack of canonical secondary structures observed in CD studies, as is often reported, determined an important loss in water solubility. In addition, the presence of the naphthyl group in the Nal1 building block can further reduce water solubility and favour stacking interactions which hamper the unambiguous assignment of NMR resonances.

The observed higher affinity of the thio-monocycle PS5(Nal1) compared to the reference compound *ic*PS5(Nal1) is likely due to enhanced aromatic interactions provided by the xylene moiety in addition to that coming from the naphthyl group of Nal1 [29]. This beneficial effect is lost in the case thio-bicycle PS5(Nal1), where the absence of the amide group of Gln at position 5, peptide numeration, subtracts spots of interactions between thio-bicycle PS5(Nal1) and JAK2, worsening the affinity. It is important to underline that additional investigations through other binding techniques (as ITC) will be required in the future to fully quantify any improvement in K_D.

Nevertheless, the insertion of the xylene scaffold did not significantly enhance the structural rigidity, as the novel compounds exhibited a slight decrease in stability to proteases when compared with the rigidity conferred by the lactam bridge in *ic*PS5(Nal1).

In conclusion, despite its limitations due to poor water solubility, the results demonstrated that the PS5 peptide is a bioactive compound with significant potential and versatility for targeted chemical modifications. This opens the path for developing KIR-SOCS1 peptidomimetics into JAK2 inhibitors.

4. Experimental

4.1. Peptide synthesis

Reagents for peptide synthesis were from Iris Biotech (Germany), solvents for peptide synthesis and HPLC analyses were from Romil (Dublin, Ireland); reversed phase columns for peptide analysis and the LC-MS system were from ThermoFisher (Waltham, MA). Linear peptides were prepared by the SPPS on a 25 μmol scale following the fluorenylmethoxycarbonyl (Fmoc) strategy as previously reported [22]. RINK AMIDE resin (substitution 0.57 mmol/g) was used as solid support [39]. The cyclization was performed by mixing crude linear peptidomimetics (1 mM) with 1.1 equivalents of α,α′-dibromo-xylene (for thio-monocycle PS5(Nal1)) or 1.1 equivalents of 1,3,5-tribromomethylbenzene (TMBM) (for thio-bicycle PS5(Nal1)) in 50 % CH_3CN and 50 % K_2HPO_4 buffer 0.1 M pH 7.6, under stirring overnight at room temperature (RT). LC-MS analysis allowed to follow cyclization: by comparing chromatographic profiles, a shift in the retention times, before and after cyclization is observable, as well as an increment of hydrophobicity of

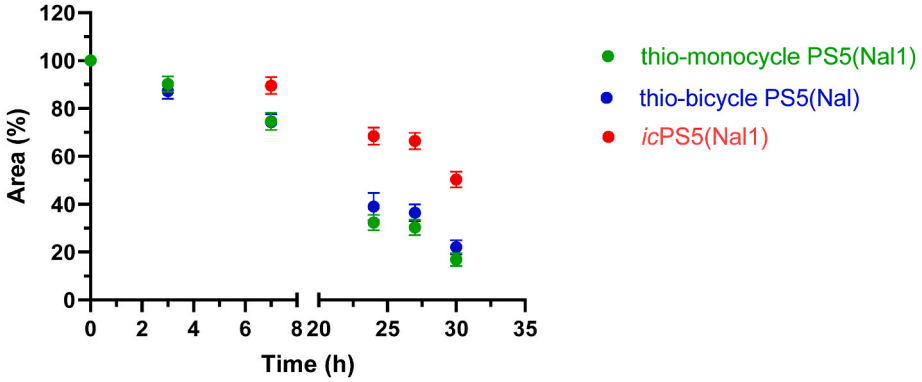

Fig. 5. Serum stability profiles of thio-cyclic analogues of *ic*PS5(Nal1). The area of chromatographic peak at t = 0 min was assumed as 100 % and residual areas at other time points were calculated as the percentage with respect to the area at t = 0 min.

the cyclic compounds and a variation in MWs (Figs. S5 and S6). In detail, the MW of the linear of bis-thio-PS5(Nal1) ($MH^+ = 1416.61$ a.m.u.) was increased by 102.13 a.m.u., corresponding to alkylated α,α′-xylene (Fig. S5 B, D), and that of the ter-thio-PS5(Nal1) ($MH^+ = 1391.62$ a.m.u.) increased by +114.14 a.m.u. corresponding to alkylated 1,3,5-trimethylbenzene (Fig. S6 B, D). The correct thiol-xylene linkage was also confirmed by NMR studies. Compounds were purified through RP-HPLC and then they were lyophilized and stored at −20 °C until use.

4.2. Microscale thermophoresis

MST experiments were performed with a Monolith NT 115 system (Nano Temper Technologies) equipped with 60 % LED and 40 % IR-laser power. Labeling of His-tagged Catalytic Domain of JAK2 (residues 826–1132) (Carna Biosciences) was achieved with the His-Tag labeling Kit RED-tris-NTA, as already reported [40]. Thio-PS5(Nal1) analogues were used starting from a stock solution of 500 μM in labeling buffer (Nano Temper Technologies); the dye concentration was adjusted to 100 nM while the protein concentration was 200 nM. Subsequently, 100 μL of protein and 100 μL of dye were incubated in the dark for 30 min. To monitor binding of cyclic analogues, a serial dilution (1:1) [41] was carried out by preparing 12–14 samples on average. Standard capillaries were employed for analysis, at 25 °C in 50 mM Tris-HCl, 150 mM NaCl, 0.05 %, Triton X-100, 1 mM dithiothreitol (DTT), 10 % glycerol, at pH 7.5. An equation implemented by the software MO-S002 MO Affinity Analysis, provided by the manufacturer, was used for fitting data at different concentrations. The equation used, is implemented by the software MO-S002 MO Affinity Analysis [42], used for fitting data at different concentrations, is:

$$f(c) = \text{Unbound} + \frac{(\text{Bound} - \text{Unbound}) \times \text{c} + \text{c(target)} + K_D - \sqrt{(c + c(target) + K_d)^2 - 4c \times c(target)}}{2c(target)} \quad (1)$$

The equation is based on Langmuir binding isotherm. In the equation "f(c)" is the fraction bound at a defined peptide concentration ("c"). "Unbound" is the F_{norm} (normalized fluorescence) signal or raw fluorescence counts (initial fluorescence mode) of the target alone (JAK2). "Bound" refers to the JAK2/peptide complex. The dissociation constant is named "K_D" and the final target concentration in the assay is indicated as "c(target)".

4.3. Inhibition of phosphorylation assay

Based on the KD values obtained from the MST experiments, the concentrations used for the phosphorylation assay were: 1) 0, 1, 10, 25, 50 μM for thio-monocycle PS5(Nal1), corresponding to range 0–2 eq and 2) 0, 1, 25, 50, 100, 150, 200 μM for thio-bicycle PS5(Nal1), corresponding, respectively, to range 0–2 and 0–8 eq with respect to the substrate Srctide (25 μM), $6{,}4 \times 10^{-3}$ eq of JAK2 (160 nM) and 64 eq of ATP (1.6 mM). Srctide peptide is a C-terminal part fragment of Src proteins, which are natural substrates of the JAK proteins [35], and its sequence is H-Gly-Glu-Glu-Pro-Leu-Tyr-Trp-Ser-Phe-Pro-Ala--Lys-Lys-Lys-NH_2. The thio-cycles and JAK2 were pre-incubated in 10 mM $MgCl_2$, 2 mM DTT 50 mM Tris-HCl pH 7.5 buffer for 1 h under stirring, at RT. Subsequently, ATP and Srctide were added to the reactions, which proceeded for 15 min. The reactions were then stopped with a 0.2 % solution of TFA in H_2O Milli-Q. The solutions were then analyzed by LC-MS and the percentages of p-Srctide were derived as a function of MS. Percentages were calculated from the area under the curve (AUC) of the non-phosphorylated Srctide peak versus the AUC of the p-Srctide peak. The relative IC_{50} was calculated for all concentrations using the function log(inhibitor) vs response -Variable slope (four parameters) by using GraphPad Prism software.

4.4. Circular dichroism (CD) spectroscopy

CD spectra were recorded on a Jasco J-810 spectropolarimeter (JASCO Corp, Milan, Italy), at 25 °C in the far UV region from 190 to 260 nm. To each spectrum (averaged on three scans) related blanks were subtracted, and the signal was reported as mean residue ellipticity in units of deg* cm^2*$dmol^{-1}$*res^{-1}. Both peptides were analyzed at 200 μM in 10 mM phosphate buffer at pH 7.4 and with a 0.1 cm path-length quartz cuvette. Deconvolutions of CD spectra were obtained by BESTSEL software (http://bestsel.elte.hu/).

4.5. NMR

NMR spectra were registered on a Bruker AVANCE 500 MHz spectrometer endowed with a Prodigy cold probe at 298 K. Peptide samples (600 μL total volumes) were prepared in 10 mM sodium phosphate buffer (NaP) with 10 % (v/v) D_2O (98 % D, Merck group/Sigma-Aldrich, Milan, Italy), and in a mixture 2,2,2-trifluoroethanol-d3 (TFE, 99.5 % isotopic purity, Merck group/Sigma-Aldrich, Milan, Italy)/NaP (50/50 v/v). Spectra recorded for both experimental conditions were: 2D [^{1}H, ^{1}H] TOCSY (Total Correlation Spectroscopy) [43], NOESY (Nuclear Overhauser Enhancement Spectroscopy) [44], ROESY (Rotating frame Overhauser Enhancement Spectroscopy) [45] and DQFCOSY [46] (Double Quantum-Filtered Correlation Spectroscopy). Typical acquisition parameters were: 32–64 scans, 256 FIDs in t1, 2048 data points in t2, mixing times corresponding to 70 ms in TOCSY, 200 and 300 ms in NOESY, and 250 ms in ROESY. The Excitation Sculpting [47] sequence was exploited to get the water signal suppression. The internal TSP (Trimethylsilyl-3-propionic acid sodium salt-D4, 98 % D, Merck group/Sigma-Aldrich, Milan, Italy) (0.0 ppm) was used for the chemical shift referencing. The processing of spectra was achieved by TopSpin 4.2 (Bruker, Milan, Italy) and the analysis by the software NEASY [48] included in CARA (Computer Aided Resonance Assignments).

4.6. Serum stability

This assay was performed in triplicate. 25 % fetal bovine serum (FBS) was incubated at 37 °C for at least 15 min, then compounds were added to the serum at a concentration of 80 μM. 50 μL aliquots of the incubating mixtures were recovered at different times: 0, 3, 7, 24, 27 and 30 h, treated with 50 μL of 30 % trichloroacetic acid (TCA) and incubated at 2 °C for at least 15 min to precipitate serum proteins. The samples were subsequently centrifuged to remove serum proteins. RP-HPLC was performed on a HPLC LC-4000 series (Jasco) with UV detector using a C18-Kinetek column from Phenomenex (Milan, Italy). Gradient elution was performed at 25 °C (monitoring at 210 nm) in a gradient starting with buffer A (0.1 % TFA in water) and applying buffer B (0.1 % TFA in acetonitrile) from 5 to 70 % in 20 min.

CRediT authorship contribution statement

Alessia Cugudda: Investigation, Formal analysis. **Sara La Manna:** Methodology, Investigation. **Marilisa Leone:** Methodology,

Investigation. **Marian Vincenzi:** Methodology, Investigation. **Daniela Marasco:** Writing – original draft, Supervision, Funding acquisition, Conceptualization.

Funding sources

This work was supported by Associazione Italiana per la Ricerca sul Cancro (AIRC) grant IG 2022, Rif. 27378 (D.M.)

Declaration of competing interest

The authors declare that they have no known competing financial interests or personal relationships that could have appeared to influence the work reported in this paper.

Abbreviations

AUC	Area under the curve
CARA	Computer Aided Resonance Assignments
CD	Circular Dichroism
DQFCOSY	Double Quantum-Filtered Correlation Spectroscopy
DTT	Dithiothreitol
ic	internal cycle
IC_{50}	Half-maximal inhibitory concentration
IF	Interferons
IL	Interleukin
KIR	Kinase inhibitory region
MOA	Mechanism of action
MST	MicroScale Thermophoresis
NMR	Nuclear Magnetic Resonance
Nal	Naphthylalanine
NOESY	Nuclear Overhauser Enhancement Spectroscopy
PEGDA	Poly (ethylene glycol) diacrylate
PTK	Protein tyrosine kinase
ROESY	Rotating frame Overhauser Enhancement Spectroscopy
RT	Room temperature
SH2	Src homology 2
SOCS	Suppressor of cytokine signalling
SPPS	Solid phase peptide synthesis
STAT	Signal transducer and activator of transcription
RP-HPLC	Reverse phase high performance liquid chromatography
TCA	Trichloroacetic acid
TFE	2,2,2 trifluoroethanol
TMBM	1,3,5-tribromomethylbenzene
TOCSY	Total Correlation Spectroscopy

Appendix A. Supplementary data

Supplementary data to this article can be found online at https://doi.org/10.1016/j.ejmech.2024.117107.

Data availability

No data was used for the research described in the article.

References

[1] C.S. Whyte, E.T. Bishop, D. Ruckerl, S. Gaspar-Pereira, R.N. Barker, J.E. Allen, A. J. Rees, H.M. Wilson, Suppressor of cytokine signaling (SOCS)1 is a key determinant of differential macrophage activation and function, J. Leukoc. Biol. 90 (2011) 845–854.

[2] S. Ilangumaran, R. Rottapel, Regulation of cytokine receptor signaling by SOCS1, Immunol. Rev. 192 (2003) 196–211.

[3] J.E. Fenner, R. Starr, A.L. Cornish, J.-G. Zhang, D. Metcalf, R.D. Schreiber, K. Sheehan, D.J. Hilton, W.S. Alexander, P.J. Hertzog, Suppressor of cytokine signaling 1 regulates the immune response to infection by a unique inhibition of type I interferon activity, Nat. Immunol. 7 (2006) 33–39.

[4] W.S. Alexander, R. Starr, J.E. Fenner, C.L. Scott, E. Handman, N.S. Sprigg, J. E. Corbin, A.L. Cornish, R. Darwiche, C.M. Owczarek, T.W. Kay, N.A. Nicola, P. J. Hertzog, D. Metcalf, D.J. Hilton, SOCS1 is a critical inhibitor of interferon gamma signaling and prevents the potentially fatal neonatal actions of this cytokine, Cell 98 (1999) 597–608.

[5] J. Hadjadj, C.N. Castro, M. Tusseau, M.C. Stolzenberg, F. Mazerolles, N. Aladjidi, M. Armstrong, H. Ashrafian, I. Cutcutache, G. Ebetsberger-Dachs, K.S. Elliott, I. Durieu, N. Fabien, M. Fusaro, M. Heeg, Y. Schmitt, M. Bras, J.C. Knight, J. C. Lega, G. Lesca, A.L. Mathieu, M. Moreews, B. Moreira, A. Nosbaum, M. Page, C. Picard, T. Ronan Leahy, I. Rouvet, E. Ryan, D. Sanlaville, K. Schwarz, A. Skelton, J.F. Viallard, S. Viel, M. Villard, I. Callebaut, C. Picard, T. Walzer, S. Ehl, A. Fischer, B. Neven, A. Belot, F. Rieux-Laucat, Early-onset autoimmunity associated with SOCS1 haploinsufficiency, Nat. Commun. 11 (2020) 5341.

[6] A. Shukla, M.G.M. Khan, A.A. Cayarga, M. Namvarpour, M.M.H. Chowdhury, D. Levesque, J.F. Lucier, F.M. Boisvert, S. Ramanathan, S. Ilangumaran, The tumor suppressor SOCS1 diminishes tolerance to oxidative stress in hepatocellular carcinoma, Cancers 16 (2024).

[7] S. Ilangumaran, Y. Gui, A. Shukla, S. Ramanathan, SOCS1 expression in cancer cells: potential roles in promoting antitumor immunity, Front. Immunol. 15 (2024) 1362224.

[8] S. La Manna, I. De Benedictis, D. Marasco, Proteomimetics of natural regulators of JAK-STAT pathway: novel therapeutic perspectives, Front. Mol. Biosci. 8 (2021) 792546.

[9] D.J. Hilton, R.T. Richardson, W.S. Alexander, E.M. Viney, T.A. Willson, N.S. Sprigg, R. Starr, S.E. Nicholson, D. Metcalf, N.A. Nicola, Twenty proteins containing a C-terminal SOCS box form five structural classes, Proc. Natl. Acad. Sci. U.S.A. 95 (1998) 114–119.

[10] N.P.D. Liau, A. Laktyushin, I.S. Lucet, J.M. Murphy, S. Yao, E. Whitlock, K. Callaghan, N.A. Nicola, N.J. Kershaw, J.J. Babon, The molecular basis of JAK/STAT inhibition by SOCS1, Nat. Commun. 9 (2018) 1558.

[11] K. Doggett, N. Keating, F. Dehkhoda, G.M. Bidgood, L.G.M. Guzman, E. Leong, A. Kueh, N.A. Nicola, N.J. Kershaw, J.J. Babon, The SOCS1 KIR and SH2 domain are both required for suppression of cytokine signaling in vivo, Cytokine 165 (2023) 156167.

[12] L.O. Flowers, H.M. Johnson, M.G. Mujtaba, M.R. Ellis, S.M.I. Haider, P. S. Subramaniam, Characterization of a peptide inhibitor of Janus kinase 2 that mimics suppressor of cytokine signaling 1 function, J. Immunol. 172 (2004) 7510–7518.

[13] J. Sharma, T.D. Collins, T. Roach, S. Mishra, B.K. Lam, Z.S. Mohamed, A.E. Veal, T. B. Polk, A. Jones, C. Cornaby, Suppressor of cytokine signaling-1 mimetic peptides attenuate lymphocyte activation in the MRL/lpr mouse autoimmune model, Sci. Rep. 11 (2021) 6354.

[14] A. Jha, J. Larkin III, E. Moore, SOCS1-KIR peptide in PEGDA hydrogels reduces pro-inflammatory macrophage activation, Macromol. Biosci. 23 (2023) 2300237.

[15] D. Marasco, G. Perretta, M. Sabatella, M. Ruvo, Past and future perspectives of synthetic peptide libraries, Curr. Protein Pept. Sci. 9 (2008) 447–467.

[16] E. Lonardo, C.L. Parish, S. Ponticelli, D. Marasco, D. Ribeiro, M. Ruvo, S. De Falco, E. Arenas, G. Minchiotti, A small synthetic cripto blocking Peptide improves neural induction, dopaminergic differentiation, and functional integration of mouse embryonic stem cells in a rat model of Parkinson's disease, Stem Cell. 28 (2010) 1326–1337.

[17] S. Ponticelli, D. Marasco, V. Tarallo, R.J. Albuquerque, S. Mitola, A. Takeda, J. M. Stassen, M. Presta, J. Ambati, M. Ruvo, S. De Falco, Modulation of angiogenesis by a tetrameric tripeptide that antagonizes vascular endothelial growth factor receptor 1, J. Biol. Chem. 283 (2008) 34250–34259.

[18] S. Madonna, C. Scarponi, N. Doti, T. Carbone, A. Cavani, P.L. Scognamiglio, D. Marasco, C. Albanesi, Therapeutical potential of a peptide mimicking the SOCS1 kinase inhibitory region in skin immune responses, Eur. J. Immunol. 43 (2013) 1883–1895.

[19] N. Doti, P.L. Scognamiglio, S. Madonna, C. Scarponi, M. Ruvo, G. Perretta, C. Albanesi, D. Marasco, New mimetic peptides of the kinase-inhibitory region (KIR) of SOCS1 through focused peptide libraries, Biochem. J. 443 (2012) 231–240.

[20] S. La Manna, P.L. Scognamiglio, C. Di Natale, M. Leone, F.A. Mercurio, A. M. Malfitano, F. Cianfarani, S. Madonna, S. Caravella, C. Albanesi, E. Novellino, D. Marasco, Characterization of linear mimetic peptides of Interleukin-22 from dissection of protein interfaces, Biochimie 138 (2017) 106–115.

[21] S. La Manna, L. Lopez-Sanz, S. Bernal, L. Jimenez-Castilla, I. Prieto, G. Morelli, C. Gomez-Guerrero, D. Marasco, Antioxidant effects of PS5, a peptidomimetic of suppressor of cytokine signaling 1, in experimental atherosclerosis, Antioxidants 9 (2020).

[22] S. La Manna, L. Lopez-Sanz, M. Leone, P. Brandi, P.L. Scognamiglio, G. Morelli, E. Novellino, C. Gomez-Guerrero, D. Marasco, Structure-activity studies of peptidomimetics based on kinase-inhibitory region of suppressors of cytokine signaling 1, Biopolymers 110.5 (2018) e23082.

[23] P.L. Scognamiglio, C. Di Natale, G. Perretta, D. Marasco, From peptides to small molecules: an intriguing but intricated way to new drugs, Curr. Med. Chem. 20 (2013) 3803–3817.

[24] S. La Manna, C. Di Natale, D. Florio, D. Marasco, Peptides as therapeutic agents for inflammatory-related diseases, Int. J. Mol. Sci. 19 (2018).

[25] A. Russo, C. Aiello, P. Grieco, D. Marasco, Targeting "undruggable" proteins: design of synthetic cyclopeptides, Curr. Med. Chem. 23 (2016) 748–762.

[26] S. La Manna, L. Lopez-Sanz, S. Bernal, S. Fortuna, F.A. Mercurio, M. Leone, C. Gomez-Guerrero, D. Marasco, Cyclic mimetics of kinase-inhibitory region of Suppressors of Cytokine Signaling 1: progress toward novel anti-inflammatory therapeutics, Eur. J. Med. Chem. 221 (2021) 113547.

[27] K. Bozovicar, T. Bratkovic, Small and simple, yet sturdy: conformationally constrained peptides with remarkable properties, Int. J. Mol. Sci. 22 (2021).
[28] R. Ferrao, P.J. Lupardus, The Janus kinase (JAK) FERM and SH2 domains: bringing specificity to JAK–receptor interactions, Front. Endocrinol. 8 (2017) 71.
[29] S. La Manna, S. Fortuna, M. Leone, F.A. Mercurio, I. Di Donato, R. Bellavita, P. Grieco, F. Merlino, D. Marasco, Ad-hoc modifications of cyclic mimetics of SOCS1 protein: structural and functional insights, Eur. J. Med. Chem. 243 (2022) 114781.
[30] P.t. Hart, P. Hommen, A. Noisier, A. Krzyzanowski, D. Schüler, A.T. Porfetye, M. Akbarzadeh, I.R. Vetter, H. Adihou, H. Waldmann, Structure based design of bicyclic peptide inhibitors of RbAp48, Angew. Chem. Int. Ed. 60 (2021) 1813–1820.
[31] P. Timmerman, J. Beld, W.C. Puijk, R.H. Meloen, Rapid and quantitative cyclization of multiple peptide loops onto synthetic scaffolds for structural mimicry of protein surfaces, Chembiochem 6 (2005) 821–824.
[32] M. Jerabek-Willemsen, C.J. Wienken, D. Braun, P. Baaske, S. Duhr, Molecular interaction studies using microscale thermophoresis, Assay Drug Dev. Technol. 9 (2011) 342–353.
[33] M. Kesarwani, E. Huber, Z. Kincaid, C.R. Evelyn, J. Biesiada, M. Rance, M.B. Thapa, N.P. Shah, J. Meller, Y. Zheng, M. Azam, Targeting substrate-site in Jak2 kinase prevents emergence of genetic resistance, Sci. Rep. 5 (2015) 14538.
[34] S. Bose, S. Banerjee, A. Mondal, U. Chakraborty, J. Pumarol, C.R. Croley, A. Bishayee, Targeting the JAK/STAT signaling pathway using phytocompounds for cancer prevention and therapy, Cells 9 (2020) 1451.
[35] Y. Deng, N.L. Alicea-Velazquez, L. Bannwarth, S.I. Lehtonen, T.J. Boggon, H. C. Cheng, V.P. Hytonen, B.E. Turk, Global analysis of human nonreceptor tyrosine kinase specificity using high-density peptide microarrays, J. Proteome Res. 13 (2014) 4339–4346.
[36] A.D. de Araujo, H.N. Hoang, W.M. Kok, F. Diness, P. Gupta, T.A. Hill, R.W. Driver, D.A. Price, S. Liras, D.P. Fairlie, Comparative alpha-helicity of cyclic pentapeptides in water, Angew Chem. Int. Ed. Engl. 53 (2014) 6965–6969.
[37] N.M. Valenzuela, JAKinibs prevent persistent, IFNγ-autonomous endothelial cell inflammation and immunogenicity, Am. J. Physiol. Cell Physiol. 325 (2023) C186–C207.
[38] M. Lin, S. Lei, Y. Chai, J. Xu, Y. Wang, C. Wu, H. Jiang, S. Yuan, J. Wang, J. Lyu, Immunosuppressive microvesicles-mimetic derived from tolerant dendritic cells to target T-lymphocytes for inflammation diseases therapy, J. Nanobiotechnol. 22 (2024).
[39] G.B. Fields, R.L. Noble, Solid phase peptide synthesis utilizing 9-fluorenylmethoxycarbonyl amino acids, Int. J. Pept. Protein Res. 35 (1990) 161–214.
[40] F.A. Mercurio, C. Di Natale, L. Pirone, R. Iannitti, D. Marasco, E.M. Pedone, R. Palumbo, M. Leone, The Sam-Sam interaction between Ship2 and the EphA2 receptor: design and analysis of peptide inhibitors, Sci. Rep. 7 (2017) 17474.
[41] F.A. Mercurio, D. Marasco, C. Di Natale, L. Pirone, S. Costantini, E.M. Pedone, M. Leone, Targeting EphA2-sam and its interactome: design and evaluation of helical peptides enriched in charged residues, Chembiochem 17 (2016) 2179–2188.
[42] L. Hellinen, S. Bahrpeyma, A.K. Rimpela, M. Hagstrom, M. Reinisalo, A. Urtti, Microscale thermophoresis as a screening tool to predict melanin binding of drugs, Pharmaceutics 12 (2020).
[43] C. Griesinger, G. Otting, K. Wüthrich, R.R. Ernst, Clean TOCSY for proton spin system identification in macromolecules, J. Am. Chem. Soc. 110 (1988) 7870–7872.
[44] R. Ernst, K. Wüthrich, A two-dimensional nuclear Overhauser enhancement (2D NOE) experiment for the elucidation of complete proton-proton cross-relaxation networks in biological macromolecules, Biochem. Biophys. Res. Commun. 95 (1980) 1–6.
[45] A. Bax, D.G. Davis, Practical aspects of two-dimensional transverse NOE spectroscopy, J. Magn. Reson. 63 (1985) 207–213.
[46] U. Piantini, O. Sorensen, R.R. Ernst, Multiple quantum filters for elucidating NMR coupling networks, J. Am. Chem. Soc. 104 (1982) 6800–6801.
[47] T.-L. Hwang, A. Shaka, Water suppression that works. Excitation sculpting using arbitrary wave-forms and pulsed-field gradients, J. Magn. Reson., Ser. A 112 (1995) 275–279.
[48] C. Bartels, T.-h. Xia, M. Billeter, P. Güntert, K. Wüthrich, The program XEASY for computer-supported NMR spectral analysis of biological macromolecules, J. Biomol. NMR 6 (1995) 1–10.